Emulsion processing of SOFC materials $Ca_{0.3}La_{0.7}CrO_3$, $Sr_{0.16}La_{0.84}CrO_3$, and $Sr_{0.2}La_{0.8}MnO_3$

J. OVENSTONE, C. B. PONTON
Department of Metallurgy and Materials Science, Birmingham University, Birmingham, UK, B15 2TT
E-mail: ovenstone99@yahoo.com

A novel preparation route to the perovskite materials $Ca_{0.3}La_{0.7}CrO_3$, $Sr_{0.16}La_{0.84}CrO_3$, and $Sr_{0.2}La_{0.8}MnO_3$ is described. The method produces the phase pure perovskite phases after calcination at 700°C for 2 hours. The powders produced are unagglomerated, and consist of hollow spherical particles 0.15 μm in diameter. EDX has shown that the careful control of reaction conditions is vital to control the phase composition, and that small changes in stoichiometry result in the production of unsinterable powder. © *2000 Kluwer Academic Publishers*

1. Introduction

There has been considerable research afforded to the synthesis and sintering of doped lanthanum chromite [1–7] and lanthanum manganite [8–10] due to their use as interconnect and cathode materials respectively in solid oxide fuel cells [11]. Despite the difficulties of fabrication, lanthanum chromite is the usual material of choice for the interconnect of ceramic fuel cells, since it is one of the few materials which can tolerate the extremely harsh operating conditions. This material is, however, notoriously difficult to sinter, since a slight excess of either the chromium or lanthanum in the ABO_3 perovskite structure results in the formation of secondary phases, which inhibit sintering [12, 13]. A slight excess of chromium can result in the volatilisation of Cr_2O_3, which then coats the surfaces of the grains, preventing further neck growth. On the other hand, an excess of lanthanum can result in the formation of localised patches of lanthanum oxide, which can then hydrate in air, causing a large expansion in the lattice parameters of the crystal, and crumbling of the ceramic. Lanthanum manganite is the most commonly used cathode material, due to its resilience in oxidising atmospheres, as well as its high electrical conductivity coupled with low ionic conductivity at high temperatures.

Emulsions consist of tiny droplets of either oil in water (o/w) or water in oil (w/o). They are usually stabilised by the addition of a surfactant, which lowers the interfacial tension between the two phases, preventing coagulation, and destabilisation. There is a vast choice of surfactants available commercially, each with its own characteristic properties, and many ways of creating the emulsion, such as rapid agitation, or as in the current project, the use of ultrasound. Emulsions have been shown to be capable of producing very fine ceramic powders, with spherical morphology which is desirable for sintering ceramic powders to high densities [14, 15]. The spherical morphology comes from the shapes of the droplets in the emulsion, which act as tiny microreactors, allowing reactant mixing on the atomic scale, but also the production of discrete powder particles due to the isolation of the droplets from each other. In the current research, the use of emulsions has been investigated for the purpose of producing sinterable perovskite powders for the ceramics $Ca_{0.3}La_{0.7}CrO_3$, $Sr_{0.16}La_{0.84}CrO_3$, and $Sr_{0.2}La_{0.8}MnO_3$ for use in solid oxide fuel cells.

2. Experimental

Metal nitrate salts were mixed into aqueous solution (50 ml) with the metal ions in the correct proportions to give solutions of the desired stoichiometry for CLC ($Ca_{0.3}La_{0.7}CrO_3$); SLC ($Sr_{0.16}La_{0.84}CrO_3$); and SLM ($Sr_{0.2}La_{0.8}MnO_3$). In some reactions, base (ammonia) was added to the aqueous reaction mixture such that the solution was 0.5 M with respect to the base. A surfactant (Span 20; sorbitan monolaurate (9.6 g)) was dissolved into kerosene (100 ml). In some cases the kerosene was replaced by heptane. The two phases (organic and aqueous) were mixed thoroughly using a magnetic stirrer before the mixture was sonicated using an ultrasonic probe (Jencons VCX 600 High Intensity Ultrasonic Processor), operating at 40% of its maximum output (600 watts). The ultrasound was pulsed such that it was on for one second and then off for two seconds repeatedly. The total time on was equivalent to 896 seconds, per litre of mixture, which was a time optimised to give the most stable emulsion during earlier trial experiments. Mixing was continued throughout this process. After treatment with ultrasound, the mixture, which had formed a water in oil (w/o) emulsion, was dropped into a hot kerosene bath, held at a constant temperature (130°C or 150°C ($\pm$2°C)), and

mixed thoroughly to ensure good heat distribution. After all the emulsion was added to the hot bath, the bath was allowed to cool to room temperature. The resulting kerosene/surfactant/powder mixture was then added to a volume of ethanol double that of the kerosene, and then spun in a centrifuge at 2500 rpm for 20 minutes. The solvent was then decanted from the powder, and the product dried in an oven at 160°C for 48 hours. The dried products were then ground, lightly, in a mortar and pestle, before calcination for two hours at 700°C in a furnace, to give the final, crystalline, solid solution perovskite powder. This is lower than the conventional temperatures required to obtain the solid solutions (800–1000°C for 8 hours), probably due to the extremely fine size of the particles which make up the hollow spheres of the powder.

The powders were dry pressed, uniaxially, into pellets of diameter 1 cm, and thickness 3 mm, by a force of 350 MPa, before being sintered for two hours in air at temperatures of 1600°C and 1450°C, respectively, for the lanthanum chromite and lanthanum manganite samples. The powders were analysed both before and after calcination using powder X-ray diffraction (XRD), differential thermal analysis (DTA), field emission gun scanning electron microscopy (FEG SEM), transmission electron microscopy (TEM), selected area diffraction (SAD), and energy dispersive X-ray analysis (EDX). The as-synthesised powders were also analysed using a Brookhaven XDC particle size analyser. Yields were calculated as percentages of the theoretical yield after calcination of samples at 1000°C for 2 hours.

3. Results and discussion

Tables I–III show the results for the emulsion syntheses of calcium doped lanthanum chromite (CLC), strontium doped lanthanum chromite (SLC) and strontium doped lanthanum manganite (SLM), respectively.

TABLE I Results for SLC reactions

Experiment	Oil bath temp (°C)	Base	Bath type	Yield (%)	Density (%)
C1	150	NH$_3$	kerosene	86.9	86
C3	150	NONE	kerosene	62.2	91
C13	130	NONE	kerosene	69.8	79
C14	130	NH$_3$	kerosene	39.5	—
C23	130	NH$_3$	heptane	42.8	—
C26	150	NH$_3$	heptane	60.3	75
C29	150	NONE	heptane	70.3	77
C39	130	NONE	heptane	42	—

TABLE II Results for CLC reactions

Experiment	Oil bath temp (°C)	Base	Bath type	Yield (%)	Density (%)
C5	150	NONE	kerosene	74	—
C16	130	NONE	kerosene	90.3	70
C24	130	NH$_3$	kerosene	41.3	—
C25	150	NH$_3$	heptane	62.2	50
C31	150	NH$_3$	kerosene	49	—
C32	150	NONE	heptane	69	62
C37	130	NH$_3$	heptane	43	—
C38	130	NONE	heptane	39	—

TABLE III Results for SLM reactions

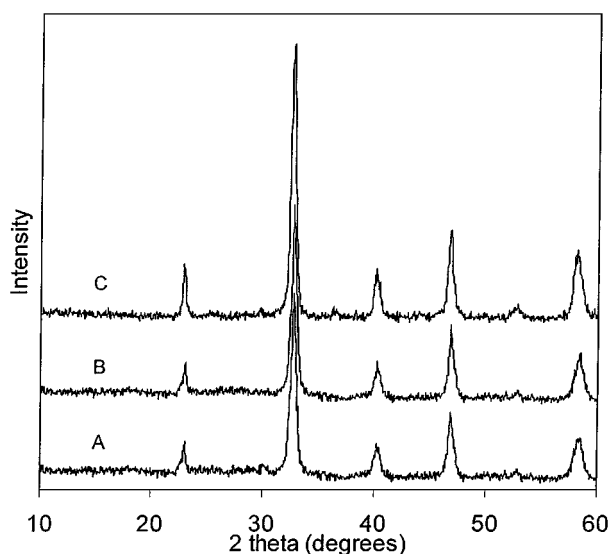| Experiment	Oil bath temp (°C)	Base	Bath type	Yield (%)	Density (%)
C11	150	NONE	kerosene	93	88
C19	130	NONE	kerosene	79.6	93
C20	130	NH$_3$	kerosene	71.7	70
C21	150	NH$_3$	kerosene	65	65
C33	150	NONE	heptane	50.3	60
C34	130	NONE	heptane	55.6	62
C35	150	NH$_3$	heptane	50.4	65
C36	130	NH$_3$	heptane	51.3	59

Figure 1 XRD traces for kerosene based emulsion produced powders after calcination at 700°C for 2 hours. (A) represents SLC (reaction C1); (B) represents CLC (reaction C16); (C) represents SLM (reaction C11).

XRD of the products after drying in the oven showed that the powders were amorphous before calcination. The XRD traces in Fig. 1 show the products of the emulsion synthesised powders after calcination at 700°C. The powders are clearly highly crystalline, and free from impurities. The SEM micrographs in Fig. 2 show the same products. In all three cases the powders produced showed a similar hollow sphere microstructure, with a particle diameter of around 0.2 μm for the doped lanthanum chromite, and around 0.8 μm for the doped lanthanum manganite.

The powders' microstructure is a direct consequence of the initial emulsion, since the precursor salts were held within the spherical droplets of aqueous phase in the emulsion. As the emulsion is dropped into the hot oil bath, the water is rapidly evaporated, carrying the precursors to the outer edges of the droplets as it expands and evaporates. As the gaseous phase is formed at the edges of the droplets, the precursors precipitate as well mixed amorphous solid salts in the shape of the droplet, thus forming a hollow sphere, with holes which allow the evaporating water in the centre of the sphere to escape. The size of the sphere is therefore directly related to the size of the initial aqueous droplet size in the emulsion. This means that the particle size of the product can be directly controlled, since the droplet size can be adjusted by careful control of the following
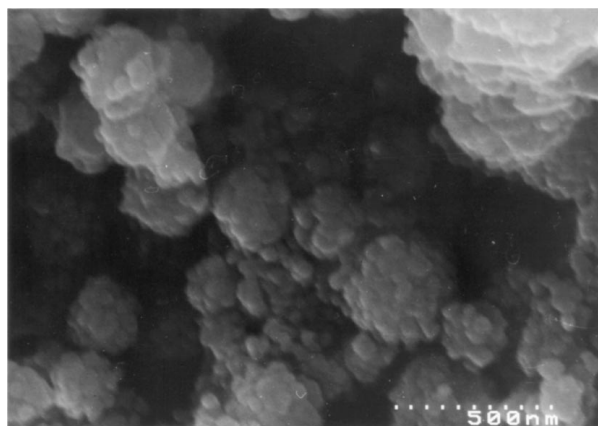
(A)
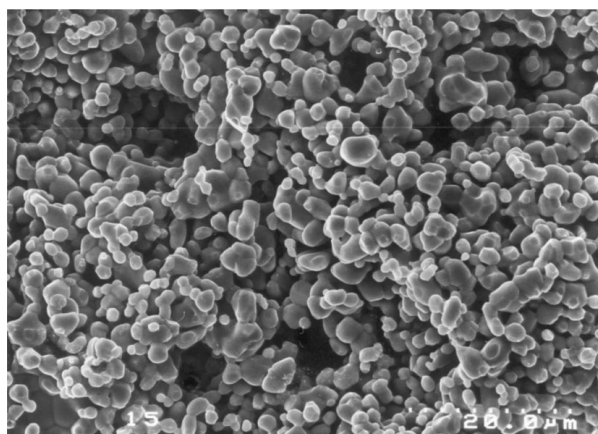
(B)
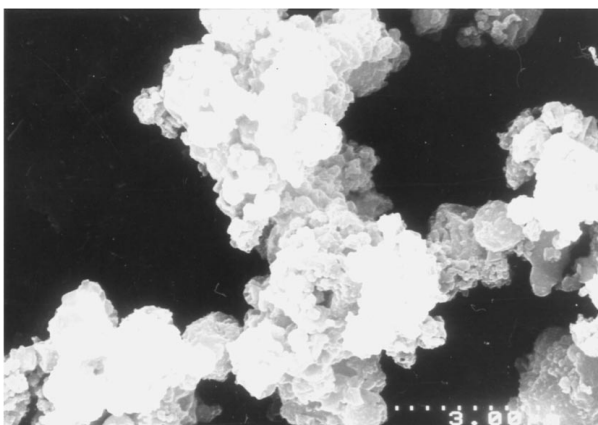
(C)

Figure 2 SEM micrographs of the powders (A) SLC (reaction C1); (B) CLC (reaction C16); (C) SLM (reaction C11) showing the spherical microstructure of the product powders after calcination.

parameters:- 1) the organic to aqueous phase ratio; 2) surfactant concentration; 3) precursor salt concentration; 4) time of ultra-sonication; 5) power of the ultra-sonic probe; 6) control over the ultra-sonic pulse cycle.

Since the aqueous phase contained all the precursors homogeneously mixed on the atomic scale, the rapid precipitation of all the precursor material in each droplet ensured that the precipitated precursors remained thoroughly mixed without regions of differing concentration due to differing precipitation rates, as is common in other ceramic synthetic routes such as co-precipitation and sol-gel. This factor is particularly important in materials such as doped lanthanum chromite, since small excesses of either the A or B site

cations in the ABO_3 perovskite structure can result in extremely bad sintering properties, as discussed earlier. The use of heptane as the organic solvent failed to produce powders with as consistently high a yield and sintered density as the powders produced when kerosene was the organic solvent. This is due to the poor temperature control as the heptane emulsions were dropped into the oil bath. Since the heptane continuous phase can evaporate faster than the aqueous phase, due to its lower boiling point, the local temperature around the individual droplets droplets is lower, and the aqueous phase evaporates slower. This allows the precursors to precipitate non-homogeneously, according to their solubilities. In addition, since the continuous phase evaporates faster than the aqueous phase, the aqueous droplets have some opportunity to combine before evaporation, thus producing larger, non-uniform particles.

The temperature of the oil bath was shown to have a mixed effect on the syntheses of the different ceramics. For the CLC, and the SLM, there was very little effect for the bath temperature on the product powder, and this was reflected in the similar yields after calcination, and also the sintered densities of the pellets for powders produced using oil bath temperatures of $130°C$ and $150°C$. On the other hand, for the SLC powders, there was a significant (at least 10%) improvement in the yield of powder produced after calcination, and also an improvement in sintered density, when the higher oil bath temperature of $150°C$ was used. These improvements were due to the faster evaporation of the aqueous phase, which resulted in a more homogeneous product. In addition, increasing the volume of the oil bath helped to stabilise the temperature during the emulsion addition. This, however, had the deleterious effect of making the recovery of the solid product more difficult, since more powder can remain suspended.

The addition of base to the reaction also had a mixed effect, depending on the ceramic product. Again the effects for CLC and SLM were similar, with the yield and sinterability of the powder being reduced by the addition of base. The SLC powder, on the other hand, showed improved yield and sinterability with base addition at the high oil bath temperature of $150°C$, and again poor yield and sinterability at the low temperature of $130°C$. These effects can be explained in terms of the homogeneity of the powder produced. For the CLC and SLM powders, the addition of base causes partial precipitation of the precursors but for the SLC powder this was not a problem at the high reaction temperature.

Fig. 3 shows the fracture surfaces for pellets of strontium doped lanthanum chromite ceramic sintered at $1600°C$ for two hours. It is clear that the material in the samples in Fig. 3A did not experience any significant mass transfer during sintering, and therefore did not reach high density. The lack of any grain growth is consistent with the formation of secondary phases and the volatilisation of Cr_2O_3 in the lanthanum chromite. Fig. 4 shows EDX spectra from the grain surface (4A), and the grain bulk (4B) of the same ceramic as in Fig. 3A, ground up into powder. It can be seen that the surface shows far higher chromium content than the bulk. This demonstrates that chromium is migrating to
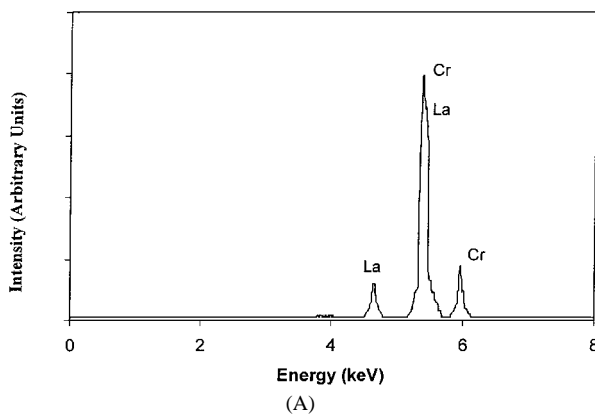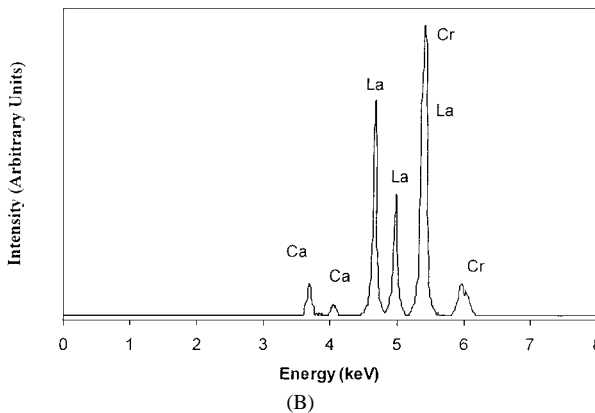
4117
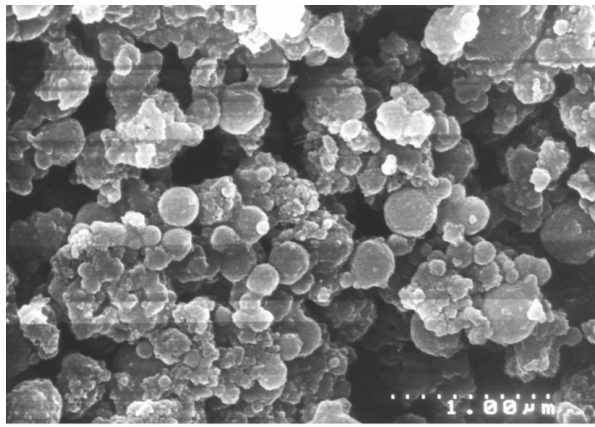
(A)
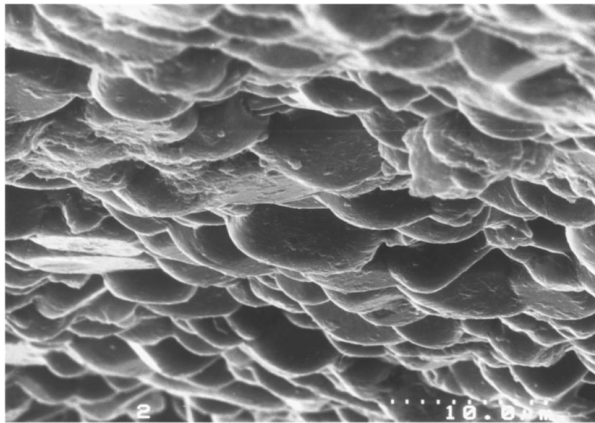
(B)

Figure 3 SEM micrographs of SLC powders sintered at 1600°C for 2 hours in air. (A) reaction C14; (B) reaction C1.


(A)

(B)

Figure 4 EDX spectra of ground, sintered SLC (reaction C14). (A) grain boundary region; (B) grain bulk.

the surface and concentrating as Cr_2O_3, as described by Meadowcroft, and explains well the poor sintering characteristics. Similar results were observed for those samples of calcium doped lanthanum chromite which did not sinter. The SEM micrograph in Fig. 3B shows a fracture surface for an SLC pellet which underwent considerable grain growth and densification. In this case, the EDX spectra for the grain surface and bulk were very similar, showing no unusual elemental concentrations. Therefore there was no hindrance, from secondary phases, to the mass transfer process during sintering.

Fig. 5 shows SEM micrographs of fracture surfaces of strontium doped lanthanum manganite pellets sintered at 1450°C for two hours. The sample shown in Fig. 5A again has not sintered well, and the particles have experienced no significant growth. This can also be explained in terms of inhomogeneity in the grains, as the EDX spectra in Fig. 6 show. Fig. 6A shows the grain boundary region, which is high in lanthanum, and low in manganese, while the grain bulk shown in Fig. 6B has a much higher proportion of manganese. This suggests that the manganese ions migrate away from the grain boundary into the bulk of the grain. This migration results in the production of a lanthanum rich region at the grain boundary, which in turn forms regions of lanthanum oxide. This oxide is then hydrated in air over time to form lanthanum hydroxide, resulting
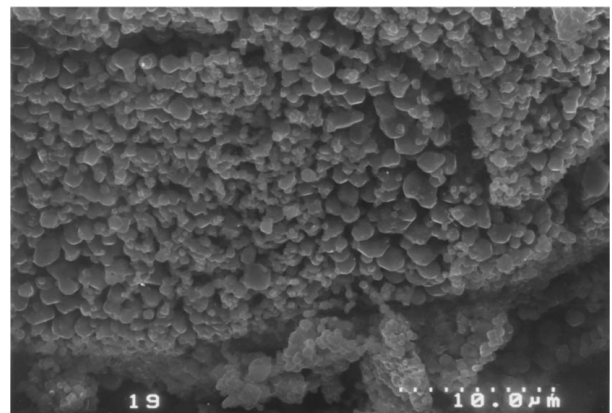
(A)
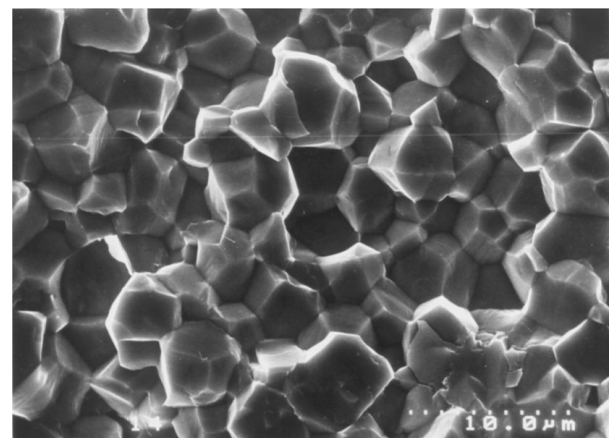
(B)

Figure 5 SEM micrographs of SLM powders sintered at 1450°C for 2 hours in air. (A) reaction C11; (B) reaction C21.
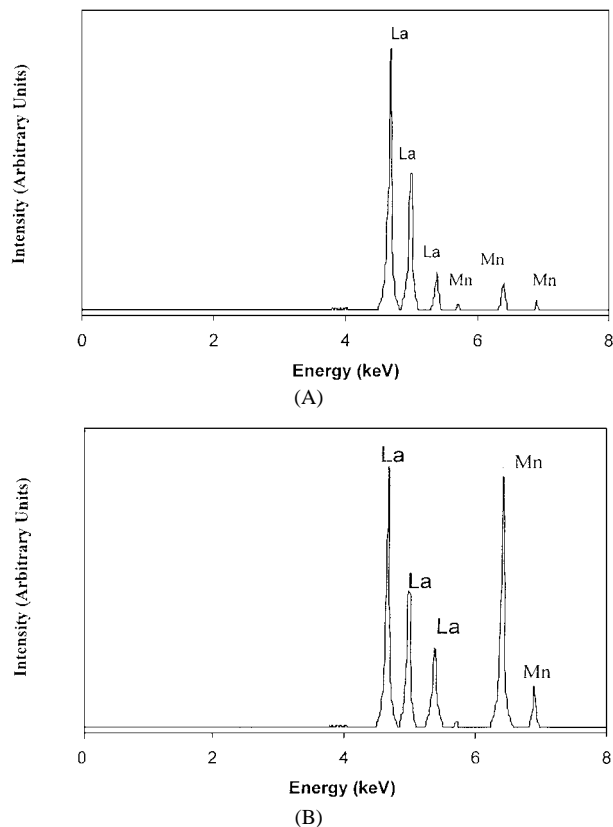
Figure 6 EDX spectra of ground, sintered SLM (reaction C21). (A) grain boundary region; (B) grain bulk.

in the crumbling of the sintered ceramic. As with the doped lanthanum chromite, the samples which sintered well, and experienced significant grain growth (Fig. 5B) showed no regions of high concentrations of particular elements.

4. Conclusions

A new method of synthesis has been attempted for the three perovskite ceramics calcium doped lanthanum chromite, strontium doped lanthanum chromite and strontium doped lanthanum manganite. Fine unagglomerated ceramic powders have been produced, with hollow spherical particle morphology. Solid solutions can be formed at temperatures as low as 700°C for 2 hours, eliminating the formation of hard agglomerates. The powders have been sintered to high densities after dry pressing at 350 MPa. The effects of the experimental variables on the final products has been discussed.

References
1. G. M. CHRISTIE, P. H. MIDDLETON and B. C. H. STEELE, *J. Europ. Ceram. Soc.* **14** (1994) 163.
2. M. R. DEGUIRE, S. E. DORRIS, R. B. POEPPEL, S. MORISETTE and U. BALACHANDRAN, *J. Mater. Res.* **8**(9) (1993) 2327.
3. P. H. DUVIGNEAUD, P. PICATE and F. CAMBIER, *J. Europ. Ceram. Soc.* **14** (1994) 359.
4. K. FUKAYA, S. HAYASHI and H. SAITO, *J. Mater. Sci. Lett.* **7** (1988) 457.
5. R. KOC and H. U. ANDERSON, *J. Mater. Sci.* **27** (1992) 5837.
6. N. SAKAI, T. KAWADA, H. YOKOKAWA and M. DOKIYA, *J. Ceram. Soc. Jap.* **101**(11) (1993) 1195.
7. N. SAKAI, T. KAWADA, H. YOKOKAWA, M. DOKIYA and I. KOJIMA, *J. Am. Ceram. Soc.* **76**(3) (1993) 609.
8. Y. TAKEDA, Y. SASAKI, T. ICHIKAWA, N. IMANISHI, O. YAMAMOTO, N. MORI and T. ABE, *Solid State Ionics* **72** (1994) 257.
9. A. CHAKRABORTY, P. SIYATHADEVI and H. S. MAITI, *Mater. Lett.* **20** (1994) 63.
10. J. H. KUO, H. U. ANDERSON and D. M. SPARLIN, *J. Solid State Chem.* **87** (1989) 52.
11. N. Q. MINH, *J. Am. Ceram. Soc.* **76**(3) (1993) 563.
12. D. B. MEADOWCROFT and J. M. WIMMER, *Ceram. Bull.* **58** (1979) 610.
13. D. B. MEADOWCROFT, *Brit. J. Appl. Phys.* **2**(2) (1969) 1225.
14. R. ARSHADY, *Colloid Polym. Sci.* **270** (1992) 717.
15. S. D. RAMAMURTHI, Z. XU and D. A. PAYNE, *J. Am. Ceram. Soc.* **73** (1990) 2760.